# Internal friction of hydrated soda-lime-silicate glasses

S. Reinsch, R. Müller, J. Deubener, and H. Behrens

Citation: The Journal of Chemical Physics **139**, 174506 (2013); doi: 10.1063/1.4828740
View online: http://dx.doi.org/10.1063/1.4828740
View Table of Contents: http://scitation.aip.org/content/aip/journal/jcp/139/17?ver=pdfcov
Published by the AIP Publishing

# Internal friction of hydrated soda-lime-silicate glasses

S. Reinsch,[1] R. Müller,[1] J. Deubener,[2] and H. Behrens[3]
[1]*BAM Federal Institute for Materials Research and Testing, 12489 Berlin, Germany*
[2]*Institute of Non-Metallic Materials, Clausthal University of Technology, 38678 Clausthal-Zellerfeld, Germany*
[3]*Institute of Mineralogy, Leibniz University of Hannover, 30167 Hannover, Germany*

(Received 16 August 2013; accepted 21 October 2013; published online 6 November 2013)

The internal friction of hydrated soda-lime-silica glasses with total water content ($C_W$) up to 1.9 wt. % was studied by dynamic mechanical analysis (DMA) using temperature-frequency sweeps from 723 K to 273 K and from 1 $s^{-1}$ to 50 $s^{-1}$. Total water content and concentrations of $H_2O$ molecules ($C_{H_2O}$) and OH groups ($C_{OH}$) in the DMA specimens were determined by infrared spectroscopy. For low water contents ($C_W \approx C_{OH} < 0.25$ wt. %) two discrete internal friction peaks below the glass transition ($\alpha$ relaxation) were assigned to the low-temperature motion of alkali ions ($\gamma$ relaxation) and cooperative movements of dissimilar mobile species under participation of OH at higher temperature ($\beta_{OH}$ relaxation). For large water contents ($C_W > 1$ wt. %), where significant amounts of molecular water are evident ($C_{H_2O} > 0.15$ wt. %), however, internal friction spectra change unexpectedly: the $\beta_{OH}$ peak heights saturate and a low temperature shoulder appears on the $\beta$-relaxation peak. This emerging relaxation mode ($\beta_{H_2O}$ relaxation) was assigned to the motions of $H_2O$ molecules. $\beta_{H_2O}$ relaxation was found to be faster than $\beta_{OH}$ but slower than $\gamma$ relaxation. Activation energy of the different relaxation modes increased in the order $\gamma < \beta_{H_2O} < \beta_{OH} < \alpha$. © *2013 AIP Publishing LLC*. [http://dx.doi.org/10.1063/1.4828740]

## I. INTRODUCTION

Sub-$T_g$ relaxation phenomena have crucial impact on aging and fatigue of glass.[1–3] For multi-component glasses they were reported to cause compaction[4] and sub-critical crack growth[5,6] at room temperature, where these relaxation modes are much faster ($\tau \approx 10^0$–$10^8$ s) and decoupled from the cooperative rearrangements of the glassy network ($\tau > 10^{27}$ s).[4]

To get insights into fast relaxation processes, internal friction studies were carried out on different glass compositions, such as alkali and alkali-alkaline earth silicates and phosphates as reviewed in Roling and Ingram[7] and Zdaniewski *et al.*[8] Using free and forced oscillation methods (mostly torsion and bending of glass beams) several sub-$T_g$ relaxation modes and the relaxation of the glass network, often labeled in the order of increasing temperature as $\gamma$, $\beta$, and $\alpha$ relaxation, have been reported.[9–11] The low temperature $\gamma$ relaxation ($T_\gamma < 373$ K; $T_\gamma/T_\alpha \approx 0.38$[12]) has been assigned to motions of alkali ions[13,14] since their range of activation energies ($E_\gamma \approx 63$–$105$ kJ $mol^{-1}$) is almost independent on the nature of the glass network forming oxides and resembles that of alkali diffusivity (63–84 kJ $mol^{-1}$).[8] At higher temperatures, $\beta$ relaxation phenomena have been assigned to several mechanisms. In case of binary alkali silicate glasses, the $\beta$-peak was suggested to account for nonbridging oxygen ion movements.[8,10] On the other hand, $\beta$ relaxation was attributed to the cooperative movement of equal[15] or dissimilar mobile species such as alkali or alkali alkaline earth ions[2,7,16–18] or as the interaction between the network and clusters formed as a consequence of alkaline earth addition.[10] Reported activation energies for $\beta$ relaxation range between 94 and 217 kJ $mol^{-1}$.[7,15,16] Depending on glass composition, $\gamma$ and $\beta$ relaxation peaks may or may not occur simultaneously in internal friction measurements.[7,8] Moreover, Ryder[10] and Shelby[16,17] reported for alkali alkaline-earth silicate and mixed alkali silicate glasses, respectively, the simultaneous occurrence of 3 peaks: $\gamma$ and two $\beta$ relaxation maxima. In these cases, one $\beta$ peak was attributed to nonbridging oxygen ion movements while the second $\beta$ peak was explained either as a cooperative movement of mobile species[16,17] or as interaction between the network and alkaline earth induced clusters.[10] As the temperature further increases, relaxation of the glass network results in a broad internal friction peak, which dominates the relaxation spectra. This $\alpha$ relaxation is characterized by relative large activation energies ($E_\alpha \approx 419$–$502$ kJ $mol^{-1}$),[8] which are in agreement with those of viscosity at $T_g$.

As water decisively influences the glass transition temperature[19–21] and kinetic fragility,[22] it also affects internal friction. Thus, Coenen[2] found $\beta$ relaxation peaks in hydrated sodium disilicate glasses (total water content $C_W \approx 0.059$ wt. %). Since the $\beta$ peak was absent in sodium diborate glasses (total water content $C_W \approx 0.054$ wt. %), a new type of $\beta$ relaxation was proposed originating from interaction of $Na^+$, non-bridging oxygens (NBO), and protons in hydrogen bonded bridging positions.[2,8] However, $\beta$ relaxation was also found in fully polymerized 25 $Li_2O$ - 25 $Al_2O_3$ - 50 $SiO_2$ glasses after partial exchange of protons for lithium[23] indicating that NBOs are not necessarily required for $\beta$ relaxation. This mechanism was therefore solely attributed to cooperative movements of $Li^+$ and $H^+$ ions.[23] Based on these findings and internal friction studies on numerous other water-poor glasses (water is predominantly present as OH groups) such as $NaPO_3$ ($C_W \approx 0.016$–$0.330$ wt. %),[24] 18 $Na_2O$ - 82 $SiO_2$

 

($C_W \approx 0.005$–$0.07$ wt. %),[25] "wet" (in air) molten $B_2O_3$,[26] proton exchanged 33 $Na_2O$ - 67 $SiO_2$,[27] and 50 $Al_2O_3$ - 50 $NaPO_3$ glasses ($C_W \approx 0.016$–$0.332$ wt. %), Day[28] concluded that $\beta$ relaxation is caused by cooperative movements of alkali ions and neighboring protons. This explanation extends the analogy to the interpretation of $\beta$ relaxation in mixed-alkali or alkali alkaline earth glasses mentioned above.

In contrast, and to the best of our knowledge, the effect of molecular water on sub-$T_g$ relaxation in glasses has not been studied. Therefore the paper aims in establishing connection between $\beta$ relaxation and water speciation. Water is known to be present in glasses as $H_2O$ molecules and OH groups. Hydration of an initially "dry" glass increases the fraction of $H_2O$ molecules due to the interconversion reaction: $H_2O + O^0 = 2\ OH$, where $O^0$ refers to a bridging oxygen and OH represents an OH-group attached to the silicate network.[29] In hydrated soda-lime-silicate glasses $C_{H_2O}$ can be detected by infrared spectroscopy for $C_W \geq 0.5$ wt. %.[30,31] Thus, in the present study soda-lime-silicate glasses in a wide range of water contents ($C_W \approx 0.015$–$1.9$ wt. %) were prepared to reveal a possible effect of $H_2O$ molecules on internal friction.

## II. EXPERIMENTAL

### A. Glass preparation

An anhydrous 74 $SiO_2$ - 16 $Na_2O$ - 10 CaO base glass (mol. % batch) was melted from $Na_2CO_3$, $CaCO_3$ (Merck p.a.) and quartz sand (Jota, Grade 6) in a Pt-crucible in an electrical furnace at 1833 K. The melt was then casted on steel molds and cooled to room temperature.

Glasses with water content up to 0.25 wt. % were obtained from base glass by remelting and water steam bubbling in 110 ml alumina crucibles at 1753 K and elevated pressure up to 3 h. For pressure melting an inductively heated 6 kW pressure furnace (BAM, Germany) was used, in which up to 0.7 MPa Ar atmospheres could be adjusted while water steam bubbling was performed with a Pt-capillary. After reducing temperature to 50 K below $T_g$ at 1 K min$^{-1}$, the melt cooled freely after pressure release by switching off the heating power.

Glasses with higher water contents ($C_W > 1$ wt. %) were prepared by re-melting base glass powders and defined amounts of water in an internally heated gas pressure vessel at about 1523 K and at pressures between 100 and 500 MPa according to Behrens and Stuke.[30] For doing so, about 1 g of glass powder was inserted stepwise into Pt-capsules ($\varnothing \approx 6$–$8$ mm, $l \approx 30$–$40$ mm). After each step the powder was compacted using a steel piston and defined portions of water were injected using a syringe. The capsule was sealed by arc-welding and checked for possible leakage by measuring the weight-change after drying at 378 K.

Bars of water-enriched and base glasses were then cut and polished to different geometry for dynamic mechanical analysis ($30 \times 5 \times 2$ mm$^3$), infrared spectroscopy (plates about $6 \times 6$ mm$^2$ with different thickness), and horizontal dilatometry ($25 \times 3 \times 3$ mm$^3$), respectively.

### B. Infrared spectroscopy

Total water concentration $C_W$ of bubbled glasses was measured using a vacuum Fourier transform infrared (FTIR) spectrometer (IFS 66v, Bruker, Ettlingen, Germany) applying the two-band method recommended by the Technical Committee (TC) 14 of the International Commission on Glass (ICG).[32] Sample homogeneity was checked by IR microscopy (IR-scope I, coupled to the IFS 66v). See Peuker *et al.*[33] for details.

$C_W$ of high pressure fused samples was determined using a Bruker IFS88 FTIR spectrometer connected to an IR microscope. In the mid-infrared $C_W$ was derived from the peak height of the band at 2850 cm$^{-1}$ with the practical absorption coefficient of $50.8 \pm 2.0$ l mol$^{-1}$ cm$^{-1}$ following the approach developed by Behrens and Stuke.[30] Additionally, absorption spectra were recorded after the dynamic mechanical analysis (DMA) experiments in the near-infrared, and water species concentrations, $C_{OH}$ and $C_{H_2O}$, were determined from the peak heights at 4500 cm$^{-1}$ and 5200 cm$^{-1}$, respectively, as described by Stuke *et al.*[31] In these measurements the sum of $C_{OH}$ and $C_{H_2O}$ revealed the total water content $C_W$. The density of high pressure fused glass samples was estimated with $\rho$ (g l$^{-1}$) $\approx 2505$ - $14.6\ C_W$ (wt. %).[30] Errors in $C_W$, $C_{OH}$, and $C_{H_2O}$ were calculated by thickness error propagation and errors of the absorption coefficients reported in literature. The good agreement between MIR-based $C_W$ and NIR-based $C_W$ supports that water loss was negligible during the DMA experiments.

### C. Dynamic mechanical analysis

Internal friction measurements were made by DMA. The used analyzer (Gabo Eplexor 150 N, Ahlden, Germany) was operated in asymmetric three-point bending mode performing temperature-frequency sweeps at 2 N static and 1 N dynamic force. Dynamic force and displacement were measured with a 25 N force detector and an inductive displacement transducer, respectively. For a given frequency $f$ of the applied forced oscillations loss maxima of tan $\delta$ appear at certain temperatures $T_i$, which are characteristic for the different relaxation modes $i$ ($i = \alpha, \beta, \gamma$). During each DMA run, $f$ was varied at constant temperature between 1 and 50 s$^{-1}$ and temperature was stepwise decreased from 723 K to 153 K. Loss data below 273 K, however, were not considered since they could be influenced by sample surface icing when operated in air. Mechanical loss (tan $\delta$) data are mean values of at least two measurements. Reproducibility of tan $\delta$ was $< \pm 5 \times 10^{-5}$.

### D. Determination of glass transition temperature

The glass transition temperatures $T_g$ were determined by a horizontal dilatometer (404E, Netzsch, Selb, Germany) operating at a heating rate of 5 K min$^{-1}$. Additionally, glass transition temperatures for water-rich samples were estimated as $T_{gc} = {T_g}^{GN}[1.01c_G + 0.22(A_{OH} \times c_{OH} + B_{H_2O} \times c_{H_2O})] \times (c_G + A_{OH} \times c_{OH} + B_{H_2O} \times c_{H_2O})^{-1}$,[20] where ${T_g}^{GN}$ is glass transition temperature of a nominally dry glass ($C_W = 0.02$ wt. %) and $C_G = (1 - C_W)$, $C_{H_2O}$ and $C_{OH}$ are the corresponding

TABLE I. Total water $C_W$ and water species concentrations $C_{OH}$ and $C_{H_2O}$ of base glass 1 and hydrated glasses 2–5 using samples of thickness $d$ and density $\rho$ and IR absorbance at 2850 $cm^{-1}$, 4500 $cm^{-1}$, and 5200 $cm^{-1}$ (Sec. II C). Glass transition temperatures were either measured by dilatometry ($T_g$) or calculated using the water speciation data ($T_{gc}$, see Sec. II D) after Deubener *et al.*[20]

| Glass | $T_g$ (K) | $T_{gc}$ (K) | $d$ ($\mu$m) | $\rho$ ($gl^{-1}$) | $A_{2850} \times 10^3$ | $A_{4500} \times 10^3$ | $A_{5200} \times 10^3$ | $C_{OH}$ (wt. %) | $C_{H_2O}$ (wt. %) | $C_W$ (wt. %) |
|---|---|---|---|---|---|---|---|---|---|---|
| 1 | 811 | | | | | | | | | 0.0151 ± 0.0004 |
| 2 | 798 | | | | | | | | | 0.170 ± 0.004 |
| 3 | 789 | | | | | | | | | 0.243 ± 0.006 |
| 4 | 661 | … | 82 ± 2 | 2489 | 623 ± 1 | … | … | … | … | 1.09 ± 0.05 |
| | | 674 | 248 ± 2 | 2489 | … | 16.6 ± 1 | 4.8 ± 1 | 0.94 ± 0.08 | 0.15 ± 0.03 | 1.09 ± 0.09 |
| 5 | 606 | … | 255 ± 2 | 2477 | 981 ± 1 | … | … | … | … | 1.89 ± 0.09 |
| | | 619 | 255 ± 2 | 2477 | … | 24.5 ± 1 | 17.4 ± 1 | 1.40 ± 0.10 | 0.52 ± 0.05 | 1.92 ± 0.11 |

weight fractions ($c_i = C_i/100\%$) of anhydrous glass and water dissolved as $H_2O$ molecules and OH groups, respectively. $A_{OH}$ and $B_{H_2O}$ are parameters weighting the influence of hydroxyl and molecular $H_2O$ on $T_g$. For depolymerized glasses $A_{OH}$ is 30 and $B_{H_2O}$ is 5,[20] similar values for soda-lime-silica glasses were reported by Del Gaudio *et al.*[34] Uncertainty of this method is ±40 K for glasses with total water >1 wt. %.[20] Calculated and experimental $T_g$ values are in very good agreement (see Table I) supporting the internal consistency of the data.

## III. RESULTS

Table I summarizes total water, $C_W$, and water species concentrations, $C_{OH}$ and $C_{H_2O}$ as well as measured and calculated glass transition temperatures of the base glass 1 and the hydrated glasses 2–5. In agreement with the physicochemical description of water as a fluxing agent, the glass transition temperature decreased with increasing water content. Inspection of Table I revealed that $H_2O$ molecules and OH groups were evident in glasses 4 and 5. NIR spectra were not recorded on glasses 1–3, but results of Stuke *et al.*[31] indicate that $C_{H_2O}$ is $\ll 0.02$ wt. % for these glasses. Thus, for the sample set under investigation $C_{H_2O}$ increased systematically with increasing $C_W$ and reached 0.52 wt. % in glass 5.

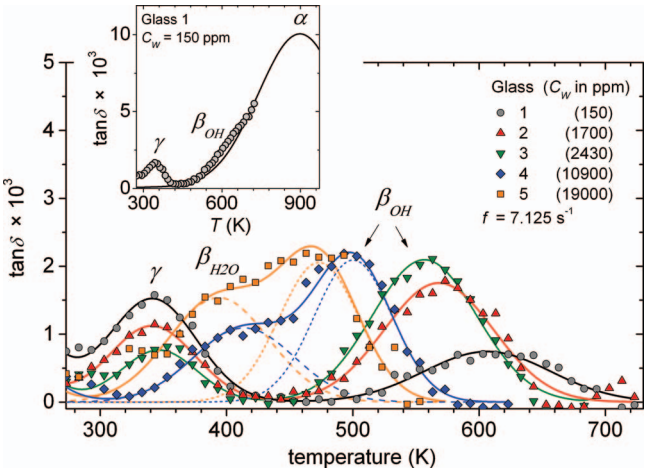


FIG. 1. Mechanical loss (tan $\delta$) vs. temperature for $f = 7.125$ $s^{-1}$ for base glass 1 and hydrated glasses 2–5. For better significance of sub-$Tg$ relaxation, the dominating contribution of $\alpha$ relaxation to tan $\delta$ is subtracted for each glass as illustrated for glass 1 (inset). Each curve is an average of several DMA runs. Dashed and dotted curves: Gaussian fits for estimation of peak temperatures and intensities of $\beta_{OH}$ and $\beta_{H_2O}$ relaxations in glasses 4 and 5.

Figure 1 exemplarily shows internal friction data for $f = 7.125$ $s^{-1}$. Although slightly shifted towards higher temperature, data for other frequencies $f$ were similar in shape and are not shown here. For better visualization of sub-$T_g$ relaxation, the dominating effect of $\alpha$ relaxation was subtracted as illustrated in the inset of Figure 1 for glass 1. For that sake, the $\alpha$ relaxation peak was modeled in terms of a Gaussian curve. Unfortunately, its maximum temperature, $T_\alpha$, cannot be measured due to the progressive viscous sample bending under the applied static load. Also, because of the frequency dependence of $\alpha$ relaxation, $T_\alpha$, cannot be simply approximated by the $T_g$ values listed in Table I. Instead, $T_\alpha$ was assumed to be the temperature at which the DMA relaxation time $\tau_{DMA} \approx 1/2\pi f$[35,36] matches the Maxwell relaxation time of viscosity

$$\tau_\eta = \frac{\eta(T_\alpha)}{G_\infty} = \tau_{DMA}, \tag{1}$$

where, $\eta$ and $G_\infty$ denote viscosity and room temperature shear modulus, respectively. For glass 1, $\eta(T)$ was calculated from VFT parameters $A = -2.462$, $B = 3950$, $T_0 = 274$ °C, and $G_\infty = 29.1$ GPa.[35] For the hydrated glasses 2–5, viscosity data reported in Ref. 34 were utilized.

Using this $T_\alpha$ value, the half-width and the amplitude of the Gaussian $\alpha$ relaxation peak was fitted to the low temperature flank of experimental tan $\delta$ data for each mechanical loss spectrum. This procedure can cause a certain inaccuracy in the determination of the $\gamma$ and $\beta$ peak temperature and height. The effect is most pronounced for the $\beta$ peak, which appears as a shoulder at the $\alpha$ relaxation (Figure 1, inset). However, variation of the fitting parameter or a direct fitting of the shoulder without subtracting the $\alpha$ peak show only small deviations in peak temperature of less than 5 K. The height may be affected stronger by this procedure because the base line is not exactly defined. Here, the lowest level of data points is used as the position of the base line. In this way the height of the peaks should become comparable relative to each other. For glasses 1–3 ($C_W < 0.25$ wt. %) the corrected internal friction data of Figure 1 clearly show two distinct relaxation peaks, which were assigned to $\gamma$ and $\beta$ modes. The $\gamma$ peak maximum $T_\gamma$ appears at ≈343 K in glass 1. With increasing water content the $\gamma$ peak decreases in height and slightly shifts towards higher temperature

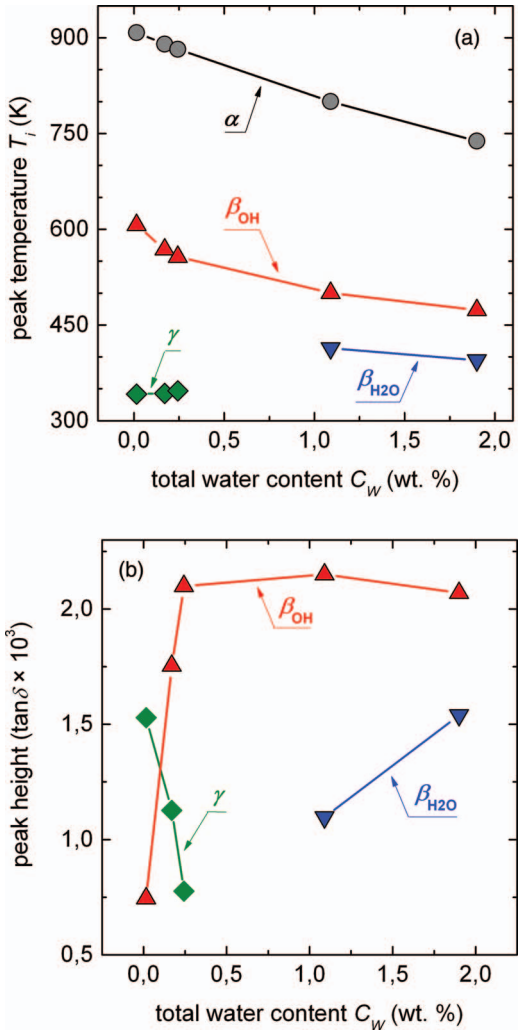


FIG. 2. Maximum temperature $T_i$ (a) and peak height (b) of DMA relaxation peaks ($\beta_{OH}$, $\beta_{H_2O}$, and $\gamma$) for $f = 7.125$ Hz of Figure 1 vs. $C_W$. $T_\alpha$ is estimated from viscosity data using Eq. (1). Lines are intended as visual guides.

(347 K) for glass 3. The $\beta$ peak behaves oppositely: $T_\beta$ shifts to lower temperature from 603 K (glass 1) to 473 K (glass 5) while its height increases with increasing water content. For $C_W > 1$ wt. % no distinct $\gamma$ peak is detectable. Instead, a pronounced low temperature shoulder of the $\beta$ peak appears for $C_W > 1$ wt. %. This new relaxation mode is assigned to the contribution of water molecules ($\beta_{H_2O}$), whereas the former was assigned to the participation of OH groups on internal friction ($\beta_{OH}$). Figure 2 illustrates these effects as a function of the water content.

## IV. DISCUSSION

For glasses 1–3 ($C_W < 0.25$ wt. %) DMA spectra are in agreement with previous literature. In particular, both the decrease of the $\gamma$ peak height and the slight increase of $T_\gamma$ with increasing water content resemble observations in previous studies on alkali and alkaline earth silicate glasses for increasing amounts of a second mobile species (e.g., other alkali ions, protons, alkaline earth ions).[8,16,37]

To relate internal friction to water speciation in glasses 1–5 and to compare the DMA results of this study with the sub-$T_g$ dynamics of other methods, the frequency dependence of the peak temperatures was considered. In particular the relaxation time of each DMA loss maximum $\tau_{DMA}$ was calculated using the simple calculus $\tau_{DMA} \approx 1/2\pi f$.[35,36] Assuming in general an Arrhenian dependence of local sub-$T_g$ relaxation processes (in contrast to the non-Arrhenian dependence of the cooperative processes of the $\alpha$ relaxation) and plotting the logarithm of the different relaxation times on an inverse temperature scale, $\tau_{DMA}$ relaxation times were assigned to $\beta_{OH}$, $\beta_{H_2O}$, and $\gamma$ relaxation modes (Figure 3). In the same way relaxation times of ultrasonic damping $\tau_{US}$,[35] and effective water diffusion $\tau_D$[38] of previous studies on glasses of the same composition were handled. Further the time scales of network relaxation $\alpha$ for glass 1 (black line A) and 5 (blue line B) were added in Figure 3 to separate the temperature-time space of the relaxed liquid from that of the unrelaxed glass (sub-$T_g$ range).[39]

From inspection of Figure 3 the following trends can be extracted: In addition to the $\alpha$-relaxation up to three contributions to the mechanical loss spectra were observed. In the glasses 1–3 where water is predominantly dissolved as OH groups, $\beta_{OH}$ and $\gamma$ relaxation were evident (lines C, G, and H). If both water species ($H_2O$ molecules and OH groups) are present in the glass, $\beta_{OH}$ and $\beta_{H_2O}$ were found (lines D, E, and F). The slope of the sub-$T_g$ relaxation lines decreased in the

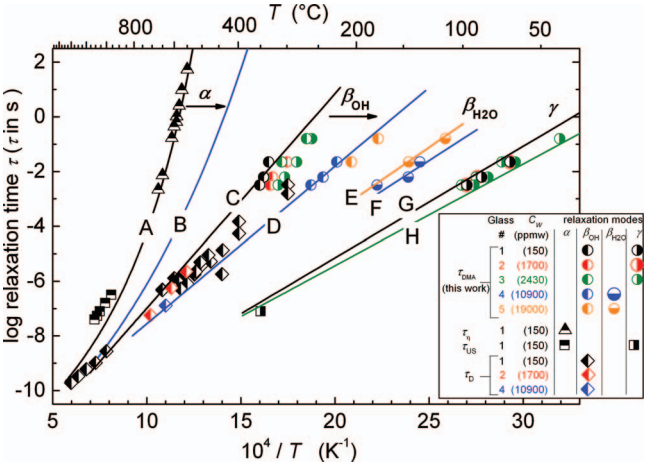


FIG. 3. Relaxation time scales in base glass 1 (74 $SiO_2$–16 $Na_2O$–10 CaO (mol. %)) and hydrated glasses 2–5 comprising relaxation times of viscosity $\tau_\eta$ (triangle),[22] ultrasound $\tau_{US}$ (square),[35] effective water diffusion $\tau_D$ (diamond),[38] and internal friction $\tau_{DMA}$ (circle) of this work. $\alpha$ relaxation: Curves A and B show $\tau_\eta$ calculated using Eq. (1) and VFT parameters of Bornhöft and Brückner[35] for glass 1 and viscosity data of Del Gaudio *et al.*[34] for glass 5, respectively. $\beta_{OH}$ relaxation: Lines C and D are fits through the DMA and diffusivity data of glass 1 ($C_W = 0.015$ wt. %) with $\tau_{\beta OH} = 1.5 \times 10^{-15}$ s exp(150 kJ mol$^{-1}$/$RT$) and glass 4 ($C_W = 1.09$ wt. %) with $\tau_{\beta OH} = 5 \times 10^{-14}$ s exp(110 kJ mol$^{-1}$/$RT$), respectively. Diffusion relaxation time $\tau_D$ was calculated from effective water diffusivity $D$ of Müller *et al.*[38] using $\tau_D \approx a^2/D$, with $D = 2 \times 10^{-6}$ m$^2$ s$^{-1}$ exp(−116 kJ mol$^{-1}$/$RT$) and $a = 300$ pm.[50] $\beta_{H_2O}$ relaxation: Line E and F are fits through the DMA data of glasses 4 ($C_W = 1.09$ wt. %) and 5 ($C_W = 1.9$ wt. %) with $\tau_{\beta H_2O} = 1 \times 10^{-13}$ s exp(91 kJ mol$^{-1}$/$RT$) and $\tau_{\beta H_2O} = 2 \times 10^{-13}$ s exp(85 kJ mol$^{-1}$/$RT$), respectively. $\gamma$ relaxation: Line G and H assign the range of $\gamma$ relaxation from DMA and ultrasonic data of glasses 1–3 ($C_W < 0.25$ wt. %) with $\tau_\gamma = 5 \times 10^{-14}$ s exp(78 kJ mol$^{-1}$/$RT$) and $\tau_\gamma = 1.4 \times 10^{-13}$ s exp(71 kJ mol$^{-1}$/$RT$), respectively. Ultrasonic relaxation time $\tau_{us}$ was calculated from damping maximum of Bornhöft and Brückner[35] using $\tau_{us} \approx 0.5\pi f$. Arrows indicate the effect of increasing water content on $\alpha$ and $\beta_{OH}$ relaxations.

order C, D, E, F, G, and H. Using $E_i = R\ln(10) \times (d\log(\tau_i/s) / d(1/T_i))$ of the relaxation modes $i$ one finds the activation energies (in kJ mol$^{-1}$): 150 ± 3 (C) and 110 ± 3 (D) for $\beta_{OH}$, 91 - 85 (E, F) for $\beta_{H_2O}$, and 78 - 71 (G, H) for $\gamma$ relaxation.

Activation energies of the $\gamma$ relaxation agreed well with those of sodium self-diffusion in soda-lime-silica glasses of similar composition ($Na_2O$/CaO in mol. %): 75 kJ mol$^{-1}$ (15.5/12.8),[40] 65 kJ mol$^{-1}$ (15.5/12.8),[41] and 95 kJ mol$^{-1}$ (15.5/10.7),[42] which further validate the assignment of the low temperature friction peak (Figure 1) with the time scale of sodium migration. The $\beta_{OH}$ peak was found to behave as previously reported for other systems as its height and temperature shift with $C_W$ oppositely compared to the $\gamma$ peak, i.e., the $\beta_{OH}$ peak height increases and its maximum temperature decreases with $C_W$ in the low water range (Figure 2). Analogous effects are well known for mixed alkali and alkali alkaline earth silicate glasses[2,8,9,11,37] as well as for low water containing 18 $Na_2O$ - 82 $SiO_2$,[25] 33 $Na_2O$ - 67 $SiO_2$,[43] $NaPO_3$,[44,45] and 50 $Al_2O_3$ - 50 $Na_2P_2O_6$ glasses[46] in which water is predominantly present as OH-groups. Further, $\beta_{OH}$ relaxation times of this study fit to the time scales of effective water diffusion and the activation energy of this relaxation mode agreed with previous findings in other glass compositions ($E_{\beta OH}$ = 126–167 kJ mol$^{-1}$).[2,7,8,10,37] As Day[28] attributed $\beta_{OH}$ relaxation to stress-induced cooperative rearrangements of alkali ions and neighbored protons, it seems likely that $\beta$ relaxation is related in the glasses of the present study to cooperative Na, Ca, and water species rearrangement mechanisms, which are decisively influenced by the water content. Since water molecules are negligible in glasses 1–3, this mechanism should mainly involve OH groups.

For $C_W > 1$ wt. % the $\beta_{OH}$ peak position decreases further from 500 to 473 K whereas the $\beta_{OH}$ relaxation peak height remains nearly constant at $C_W > 0.24$ wt. % (Figure 2). The latter effect cannot be explained if one assumes a positive correlation of the $\beta_{OH}$ relaxation peak height and $C_{OH}$ and is not expected from previous literature. For instance, Day and Stevels[24] reported a linear increase of the $\beta$ peak height in $NaPO_3$ glass with water content up to the largest water content studied (0.33 wt. %). Most notably, a pronounced shoulder appears at the low temperature flank of the $\beta_{OH}$ relaxation peak while the $\gamma$ relaxation at ≈343 K fully disappears according to the trend shown in Figure 2. The shoulder occurs at approximately 423 and 403 K for glasses 4 and 5, respectively, i.e., the temperature of the maximum of the Gaussian component (see dashed curves in Figure 1) decreases with increasing water content. This behavior and the observed strong increase in shoulder intensity with increasing water content make it difficult to attribute this shoulder to the $\gamma$ relaxation peak of alkali motion.

On the other hand, its peak position occurs well below the $\beta_{OH}$ peak, indicating a less complex relaxation mechanism. Although no strict evidence can be given here, such an effect seems rather plausible for water molecules than for structural groups related to dissociated water, which requires a more pronounced local network relaxation. Since in glasses 4 and 5 significant amounts of $H_2O$ molecules are evident the $\beta_{H_2O}$ internal friction peak is assigned to the dynamics of $H_2O$ molecules.

To discuss this assignment in the light of the present understanding of water diffusion in silicate glasses we shortly recall that depending on the number of non-bridging oxygen per network tetrahedron (NBO/T), i.e. fully polymerized vs. depolymerized glasses, two mechanisms were proposed to control the diffusion of water. In NBO-free glasses it has been proposed that $H_2O$ molecules migrate through the silicate network by direct jumps between neighboring cavities, while a reaction with a bridging oxygen immobilizes the $H_2O$ molecule.[46,47] Furthermore, a transition state for the migration of molecular water, in which the $H_2O$ molecule and the bridging oxygen (BO) forms a pair of OH groups has been suggested.[48–50] Under sub-$T_g$ condition, however, network relaxation is too slow to stabilize the extended transition state required for formation of OH pairs and to achieve equilibrium for hydrous species. Thus, under such non-equilibrium conditions the Doremus diffusion model,[51] in which $H_2O$ molecules play an important role in bulk water diffusion, works successfully. The migration of $H_2O$ molecules without or at least with minor interaction with network oxygen has been evidenced by the study of Helmich and Rauch[52] showing that below 473 K $H_2O$ molecules diffuse as an entity into silica glass (NBO/T = 0) without isotopic exchange with BO. Further evidence comes from NMR[53,54] and quasi-elastic neutron scattering experiments,[55] which demonstrate that rotation of $H_2O$ molecules around their bisector axis is active even at temperatures below 400 K. However, the dynamics of this motional process are found to be much faster ($\tau_{H_2O-rot} \approx 10^{-12}$ s at 400 K) than translatory jumps from one cavity to another.

To compare these findings with the observed $\beta_{H_2O}$ relaxation times in hydrous soda-lime-silicate glasses (NBO/T = 0.7) the motional correlation times of molecular water diffusion in silica glass of Helmich and Rauch[52] are approximated using $\tau_D \approx a^2/D$ and the jump distance $a \approx 300$ pm.[50] Figure 4 shows that $H_2O$ molecules in silica glass fit the relaxation times of the novel internal friction mode $\beta_{H_2O}$ of glasses 4 and 5.

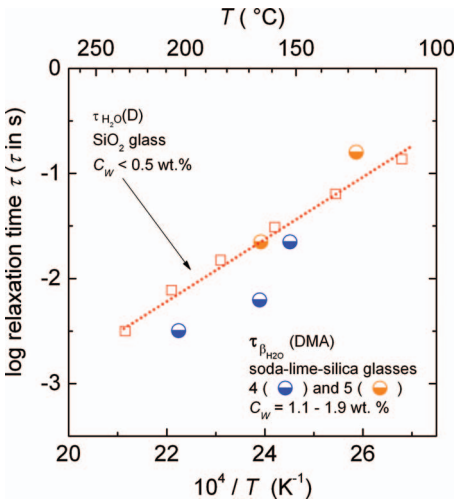


FIG. 4. Relaxation time scales of water molecules in silicate glasses: $\tau_\beta$ in soda-lime-silica glasses 4 and 5 (NBO/T = 0.7) (half-filled circles) and $\tau_{H_2O}$ in silica glass (NBO/T = 0)[52] (dotted line and open squares).

On the other hand, in glasses of high NBO concentrations, reactions with diffusing protons favor the formation of OH groups. This results in a local charge imbalance, which facilitates the attack of a diffusing OH on one of the bonds associated with the BO.[56] Thus, contributions of proton-hopping to water diffusion in hydrous silicate glasses are discussed in literature. In particular, proton conduction has been reported in hydrous barium disilicate glasses[57] and in a Ca, Mg aluminosilicate glass at water contents above 1.5 wt. %, i.e., when molecular $H_2O$ becomes more abundant.[58] However, contributions of protons on water mobility in the studied soda-lime-silica glasses are speculative since conduction measurements are lacking and the conductivity change by water addition may be also due to the change in the mobility of other mobile ions in the glass (Na, Ca) by water addition.

Nevertheless, it is clear that molecular $H_2O$ is the crucial species responsible for the $\beta_{H_2O}$ relaxation. To clarify the mechanism of this dynamic process in detail, internal friction studies are needed on hydrous glasses with low proton mobility, i.e., polymerized aluminosilicate glasses.[58]

## V. CONCLUSIONS

Internal friction of hydrous soda-lime-silica glasses seems to be correlated with water speciation. Characteristic peaks of the mechanical loss tan $\delta$ can be assigned to the time scales associated with the dynamics of both OH groups and $H_2O$ molecules. The relaxation of the $H_2O$-bearing mode is found to be faster and decoupled from the OH-based mechanism. This fast dynamic process is assigned to the jumps of $H_2O$ molecules between adjacent cavities in the network while hopping of protons between $H_2O$ molecules and nonbridging oxygens are less probable on the basis of the available data. Subsequent studies are required to confirm that assignment.

## ACKNOWLEDGMENTS

Financial support of the Deutsche Forschungsgemeinschaft (DFG) by the priority program SPP 1594 is gratefully acknowledged. S.R. and R.M. thank A. Kohl (IR spectroscopy), R. Schadrack (horizontal dilatometry), A. Marek (density), and R. Koslowski (DMA sample preparation) at BAM for experimental help.

[1]D. E. Day and G. E. Rindone, J. Am. Ceram. Soc. **44**, 161 (1961).
[2]M. Coenen, Z. Elektrochem. **65**, 903 (1961).
[3]M. Tomozawa and R. P. Hepburn, J. Non-Cryst. Solids **345–346**, 449 (2004).
[4]S. V. Nemilov, Glass Phys. Chem. **26**, 511 (2000).
[5]S. M. Wiederhorn, J. Am. Ceram. Soc. **50**, 407 (1967).
[6]M. Tomozawa, Annu. Rev. Mater. Sci. **26**, 43 (1996).
[7]B. Roling and M. D. Ingram, Phys. Rev. B **57**, 14192 (1998).
[8]W. A. Zdaniewski, G. E. Rindone, and D. E. Day, J. Mater. Sci. **14**, 763 (1979).
[9]R. J. Ryder and G. E. Rindone, J. Am. Ceram. Soc. **43**, 662 (1960).
[10]R. J. Ryder and G. E. Rindone, J. Am. Ceram. Soc. **44**, 532 (1961).
[11]R. Brückner, Glastech. Ber. **37**, 536 (1964).
[12]S. V. Nemilov, J. Non-Cryst. Solids **357**, 1243 (2011).
[13]H. von Rötger, Glastech. Ber. **19**, 192 (1941).
[14]J. V. Fitzgerald, J. Am. Ceram. Soc. **34**, 339 (1951).
[15]K. E. Forry, J. Am. Ceram. Soc. **40**, 90 (1957).
[16]J. E. Shelby and D. E. Day, J. Am. Ceram. Soc. **52**, 169 (1969).
[17]J. E. Shelby and D. E. Day, J. Am. Ceram. Soc. **53**, 182 (1970).
[18]J. W. Fleming and D. E. Day, J. Am. Ceram. Soc. **55**, 186 (1972).
[19]M. Tomozawa, M. Takata, J. Acocella, E. B. Watson, and T. Takamori, J. Non-Cryst. Solids **56**, 343 (1983).
[20]J. Deubener, R. Müller, H. Behrens, and G. Heide, J. Non-Cryst. Solids **330**, 268 (2003).
[21]S. Zietka, J. Deubener, H. Behrens, and R. Müller, Phys. Chem. Glasses: Eur. J. Glass Sci. Technol. B **48**, 380 (2007).
[22]J. Deubener, H. Behrens, R. Müller, S. Zietka, and S. Reinsch, J. Non-Cryst. Solids **354**, 4713 (2008).
[23]A. I. A. Abdel-Latif, and D. E. Day, J. Am. Ceram. Soc. **55**, 254 (1972).
[24]D. E. Day and J. M. Stevels, J. Non-Cryst Solids **11**, 459 (1973).
[25]M. S. Maklad and N. J. Kreidl, *Scientific and Technical Communications of the 9th International Congress on Glass* Vol. 1 (Institut du Verre, Paris, France, 27 September - 2 October 1971) pp. 75–100.
[26]R. E. Strakna and H. T. Savage, J. Appl. Phys. **35**, 1445 (1964).
[27]H. De Waal, J. Am. Ceram. Soc. **52**, 165 (1969).
[28]D. E. Day, Wiss. Z. - Friedrich-Schiller-Univ. Jena: Naturwiss. Reihe **23**, 293 (1974).
[29]E. Stolper, Geochim. Cosmochim. Acta **46**, 2609 (1982).
[30]H. Behrens and A. Stuke, Glass Sci. Technol. **76**, 176 (2003).
[31]A. Stuke, H. Behrens, B. C. Schmidt, and R. Dupree, Chem. Geol. **229**, 64 (2006).
[32]F. Geotti-Bianchini, H. Geissler, F. Kramer, and I. H. Smith, Glass Sci. Technol. **72**, 103 (1999).
[33]C. Peuker, U. Reinholz, C. Jagger, J. Pauli, and H. Geissler, Glass Sci. Technol. **76**, 227 (2003).
[34]P. Del Gaudio, H. Behrens, and J. Deubener, J. Non-Cryst. Solids **353**, 223 (2007).
[35]H. Bornhöft and R. Brückner, Glastech. Ber. **67**, 241 (1994).
[36]J. Deubener, H. Bornhöft, S. Reinsch, R. Müller, J. Lumeau, L. N. Glebova, and L. B. Glebov, J. Non-Cryst. Solids **355**, 126 (2009).
[37]B. Roling and M. D. Ingram, Solid State Ionics **105**, 47 (1998).
[38]R. Müller, P. Gottschling, and M. Gaber, Glass Sci. Technol. **78**, 76 (2005).
[39]D. B. Dingwell and S. L. Webb, Eur. J. Mineral. **2**, 427 (1990).
[40]J. R. Johnson, R. H. Bristow, and H. H. Blau, J. Am. Ceram. Soc. **34**, 165 (1951).
[41]C. G. Wilson and A. C. Carter, Phys. Chem. Glasses **5**, 111 (1964).
[42]G. H. Frischat, Glastech. Ber. **44**, 93 (1971).
[43]T. D. Taylor and G. E. Rindone, J. Non-Cryst. Solids **14**, 157 (1974).
[44]D. E. Day, J. Am. Ceram. Soc. **57**, 530 (1974).
[45]D. E. Day and J. M. Stevels, J. Non-Cryst. Solids **14**, 165 (1974).
[46]R. H. Doremus, *Diffusion of Reactive Molecules in Solids and Melts* (Wiley, New York, 2002), p. 74.
[47]Y. Zhang, E. M. Stolper, and G. J. Wasserburg, Earth Planet. Sci. Lett. **103**, 228 (1991).
[48]G. J. Roberts and J. P. Roberts, Phys. Chem. Glasses **7**, 82 (1966).
[49]M. Tomozawa, J. Am. Ceram. Soc. **68**, C-251 (1985).
[50]H. Behrens and M. Nowak, Contrib. Mineral. Petrol. **126**, 377 (1997).
[51]R. H. Doremus, J. Mater. Res. **10**, 2379 (1995).
[52]M. Helmich and F. Rauch, Glastech. Ber. **66**, 195 (1993).
[53]H. Eckert, J. P. Yesinowski, E. M. Stolper, T. R. Stanton, and J. Holloway, J. Non-Cryst. Solids **93**, 93 (1987).
[54]H. Eckert, J. P. Yesinowski, L. A. Silver, and E. M. Stolper, J. Phys. Chem. **92**, 2055 (1988).
[55]S. Indris, P. Heitjans, H. Behrens, R. Zorn, and B. Frick, Phys. Rev. B **71**, 064205 (2005).
[56]Z. Haider and G. J. Roberts, Glass Technol. **6**, 158 (1970).
[57]H. Behrens, R. Kappes, and P. Heitjans, J. Non-Cryst. Solids **306**, 271 (2002).
[58]S. Fanara and H. Behrens, J. Chem. Phys. **134**, 194505 (2011).